Studies on the Yield of Plastic Hinges in Concrete Beams

By

Kiyoshi OKADA* and Wataru KOYANAGI*

(Received October 31, 1963)

Experimental studies were carried out to investigate the yield of plastic hinges in reinforced and prestressed concrete beams. Eighty-eight simple beams and thirty-two two-span continuous beams were tested under static loading to failure and theoretical analysis was made as to the rotation capacity of plastic hinges and the redistribution of internal bending moments. The rotation capacities of plastic hinges were analysed using the reinforcement index q. To examine the yield of plastic hinges in continuous beams, the measured strengths of beams were compared with those calculated values based on the simple beam tests. Though a prestressed concrete beam does not show any definite yield phenomena, the plastic rotation can also be calculated just as in case of reinforced concrete beams. But the rotation capacities of the former are a good deal smaller than that of the latter. The yield of plastic hinges though partly incomplete, were recognized both in prestressed and reinforced concrete beams.

1. Introduction

Recently, the ultimate load design theory based on the assumption of the yield of plastic hinges has been applied to the design of steel structures. However, the applicability of this theory to concrete structures is still questionable, owing to the brittleness and heterogeneity of concrete properties.

To investigate the yield of plastic hinges in reinforced and prestressed concrete structures, static flexural tests of simple- and two-span continuous beams were conducted. The authors describe here the results of the experimental study mainly on the rotation capacity of plastic hinges and the redistribution of moments.

2. Rotation Capacities of Plastic Hinges

In order that the plastic hinge yields in a structure, the section should have a sufficient capacity of plastic rotation. The plastic rotation in the concrete

* Department of Civil Engineering

structure is different from that in the steel structure made of the approximately ideal elastic plastic material—mild steel.

When a reinforced concrete beam having a steel ratio of less than the balanced reinforcement is subjected to bending, the stress of steel reaches its yield point at first if the steel has a yield point, and then the section rotates remarkably until the concrete in the compression zone crushes. In this case, the moment curvature relationship is schematically shown in Fig. 1. If the work hardening of steel can be ignored, the difference of yield moment M_y and the ultimate moment M_u is negligible, and the rotation capacity of the section, that is, the total curvature of plastic rotation is given by $(\varphi_u - \varphi_e)$ in Fig. 1.

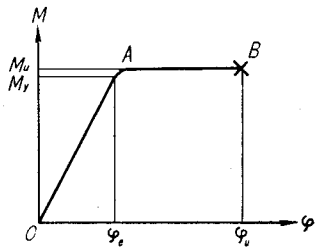

Fig. 1. Moment versus curvature relationship of reinforced concrete.

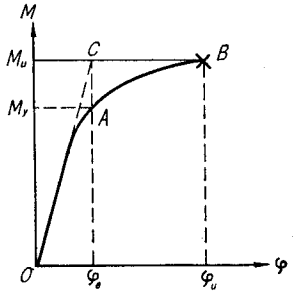

Fig. 2. Moment versus curvature relationship of prestressed concrete.

Usually in the prestressed concrete beams, however, no definite yield phenomenon can be seen as shown in Fig. 2 since the prestressing steel such as wire or strand has no definite yield point. Therefore, the yield moment M_y is defined, in this paper, as point A, in Fig. 2, of the moment-curvature curve OAB intersecting the perpendicular passing through C,—the intersecting point of the initial tangent OC and the horizontal BC having an ordinate M_u. The bending moment diagram of a simple beam in flexure by the mid span loading is given as in Fig. 3-a. The region, l_p, where bending moment exceeds the yield moment is assumed to be a plastic hinge. The curvature diagram of the section is divided into the elastic portion φ_{ex} and the plastic portion φ_{px} as shown in Fig. 3-b. The deflection diagram is also illustrated in Fig. 3-c. The rotation, θ_p, of the hinge is given as follows;

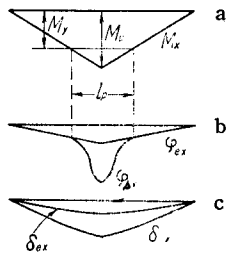

Fig. 3. Distribution of moment, curvature and deflection in simple beam.

$$\theta_p = \int_0^{l_p} \varphi_{px} dx \qquad \cdots\cdots (1)$$

$$\theta_p = 2\sum_{i=1}^{n} \frac{\Delta\delta_{px_i}}{\Delta x_i} \qquad \cdots\cdots (2)$$

where $x_n = l/2$

In practice the distribution of φ_{px} or δ_{px} in the actual beam can not be easily determined, and therefore it is assumed that the plastic rotation occurs concentratedly in the section under the loading point. Thus the plastic rotation capacity θ_p can be calculated from Eq. (2) using the ultimate plastic deflection of the loading point as follows;

$$\theta_p = 4\delta_p/l \quad \text{(mid span loading)} \qquad \cdots\cdots (3)$$

$$\theta_p = 6\delta_p/l \quad \text{(third point loading)} \qquad \cdots\cdots (4)$$

where l: span length

Theoretically speaking, the plastic rotation would occur rather concentratedly at each of the cracked sections and the hinge length would be affected by the distribution and width of cracks. It is so complicated, however, to consider these factors, that only the total plastic rotation θ_p of the hinge section l_p is taken in this study.

3. Description of Tests

3.1. Outlines of tests

Four series of tests were made. In series I and II, simple beams of reinforced and prestressed concrete were tested to determine the capacity of plastic rotation, and in series III and IV two-span continuous beams of reinforced and prestressed concrete were tested to observe in what manner and to what degree the plastic hinge developed. Scope of tests, test procedure and principal properties of specimens are listed in Table 1.

3.2. Series I-Tests for plastic rotation capacity of reinforced concrete

3.2.1. Fabrication of specimens and test procedure—In this series twenty-two kinds of specimens were tested, which were divided into four groups of A, B, C and D as given in Table 1. Variables involved are the kind, amount and arrangements of reinforcing steel, the strength of concrete, and the loading manner. In each kind of test, two specimens were used. Stirrups were provided in all of the beams to prevent shear failure.

All beams were tested by the 100 ton Riehle type universal testing machine. Strains in the concrete on the top and bottom of the loaded sections were measured with electric wire strain gages, and deflections of beams under the

Table 1. Principal properties of specimens.

Series	Group No.	Kind of reinf.	Dia. of steel (mm) Tens. side	Dia. of steel (mm) Comp. side	Steel ratios (%) p	Steel ratios (%) p'	Concrete strength kg/cm²	Dimension, Loading manner (cm)
I	A-a/A-b	Plain SS 41	2φ6 2φ9 2φ13 2φ16	—	0.44 0.98 2.04 3.11	—	200/400	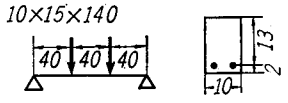
	B-a		2φ6 2φ9 2φ13	2φ6 2φ9 2φ13	0.44 0.98 2.04	0.44 0.98 2.04	200	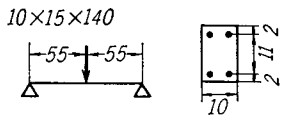
	B-b		2φ9 2φ13 2φ16	2φ9 2φ13 2φ16	0.98 2.04 3.11	0.98 2.04 3.11	400	
	C-a/C-b	P. bar SS 50	2φ16 2φ9	2φ9 2φ16	2.30 0.73	0.73 2.30	200/300	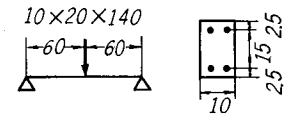
	D-a/D-b	Deformed bar SSD 49	2φ16 2φ9	2φ9 2φ16	2.26 0.81	0.81 2.26	200/300	
II	E-a/E-b	Prestressing steel bar (induction hardened)	φ10 φ14 φ14	—	0.78 1.54 1.54	—	200/400	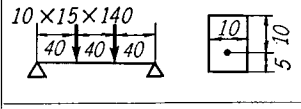
	F-a/F-b		φ10 φ12 φ14	—	0.47 0.68 0.95	—	400	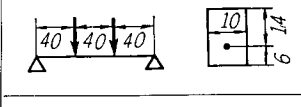
	G-a/G-b		φ10 φ10 φ12 φ10 φ14	φ10 φ12 φ10 φ14 φ10	0.44 0.44 0.64 0.44 0.89	0.44 0.64 0.44 0.89 0.44	400/300	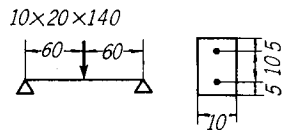
III	H-a	same as B-a						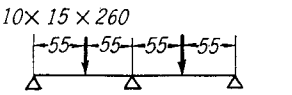
	H-b	same as B-b						
	I-a/I-b	same as C-a/C-b						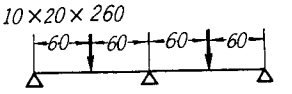
	J-a/J-b	same as D-a/D-b						
IV	K-a/K-b	same as G-a/G-b						

loading points were measured with dial gages of 1/100 mm scale. The automatic load-deflection recorder provided in the testing machine was also used in analysing the data.

3. 2. 2. Results of test—The measurements of the ultimate defiction scatter fairly much in some kinds of beams, as compared with those of the ultimate failure moments. Therefore it is inevitable that the analysis was made rather quantatively than qualitatively concerning the rotation capacity.

Index q used in analysing the results of the test, is defined by Eq. (5), and it corresponds to the neutral axis ratio at the failure of beams.

$$q = p\frac{\sigma_y}{\sigma_c} - k_c p' \frac{\sigma_y'}{\sigma_c} \qquad \cdots\cdots (5)$$

where k_c : a ratio of actual stress in compressive reinforcement to its yield stress and given by $k_c = (q-d_c')/(1-q)$

p, p' : steel ratios of tension and compression side, respectively

σ_y, σ_y' : yield stress of tension and compression steel, respectively

σ_c : compressive strength of concrete

d_c' : a ratio of covering depth to its beam depth d

The following assumptions are also made: (1) the strain distribution on the section is linear up to the beam failure, (2) the ultimate compressive stress of concrete is of rectangular distribution and (3) the ultimate strain of concrete is 0.003.

The plastic rotations θ_p were calculated from the measured plastic deflection δ_p using Eq. (3) or (4), and plotted against q in Fig. 4. In the figure two curves are drawn which are calculated by the rotation energy theory developed by Yamada[1], and given by following equations

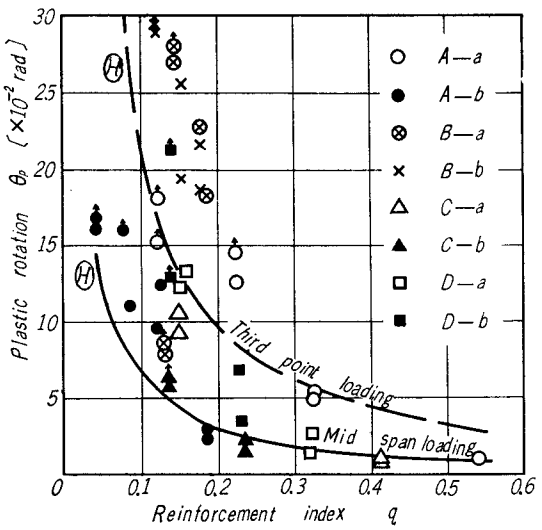

Fig. 4. θ_p versus q relationship of reinforced concrete.

$$\Theta = \frac{q^2+4(1-q)(1-q/2)}{q(1-q/2)}\cdot\varepsilon_p^* \qquad \text{(mid span loading)} \qquad \cdots\cdots (6)$$

$$\Theta = \frac{q(l/3+qd)+2(1-q)\{l/3+2(1-q/2)d\}}{q(1-q/2)d}\cdot\varepsilon_p^* \qquad \text{(third point loading)} \qquad \cdots\cdots (7)$$

where ε_p^* is the plastic strain of concrete and assumed to be 0.002.

The value of plastic rotation is larger for the higher strength of concrete, the smaller steel ratio and the lower yield point of steel. Though it is very large in the range of smaller q, it decreases remarkably with increasing q. Θ curves based on the energy theory show fairly good agreement with the measurements only in the range of q larger than 0.2 for the mid span loading.

It is observed that the plastic rotation of the beam with deformed bars (Group D) seems larger than that of the beam with plain bars (Group C).

The general trend is that the theoretical curve Θ for mid-span loading indicates nearly the minimum values of all of the measurements. Thus it may be said that q is a parameter valuable for expressing the plastic rotation but it appears that the critical rotation capacity of plastic hinges can be determined not so definitely by this parameter q only. Further studies are needed on this point.

3.3. Series II - Tests for plastic rotation capacity of prestressed concrete

3.3.1. Fabrication of specimens and test procedure—Twenty-two kinds of specimens were tested, which are divided into 3 groups of E, F and G as listed in Table 1. Variables involved are the amount of prestressing steel, the magnitude of prestress introduced, the strength of concrete and the loading manner. In all the beams, high strength bar (induction hardened) was used for prestressing.

Prestress was introduced by the post-tentioning method at age of 2 weeks and re-introduced at 3 weeks immediately followed by injection of cement paste. The effective average prestresses were chosen from 30 to 60 kg/cm^2. And the beams were tested at 5 weeks. The method of loading and measurements were nearly the same as made on the reinforced concrete beams. In strain measurment a Huggenberger strain meter (gage length 10 inches) was also used in this series.

3.3.2. Results of test—As already described above, the yield point of the prestressed concrete member was defined by point A in Fig. 2. The plastic rotation calculated from the plastic deflection from Eqs. (3) or (4) coincided very closely with the measured values. As the values of σ_c in Eq. (5), the strength obtained by $\phi 15 \times 30$ cm cylinders, minus the stress introduced by prestressing on the end fiber of the compression side of the beam, was used.

The relation between the plastic rotation and the reinforcement index is shown in Fig. 5. Doubly reinforced concrete beams (Group G) show smaller rotation as compared with the single reinforced (Group E, F) having the same value of q. However, this may be due to the influence of loading method rather than of the arrangement of reinforcement. Because in case of the third

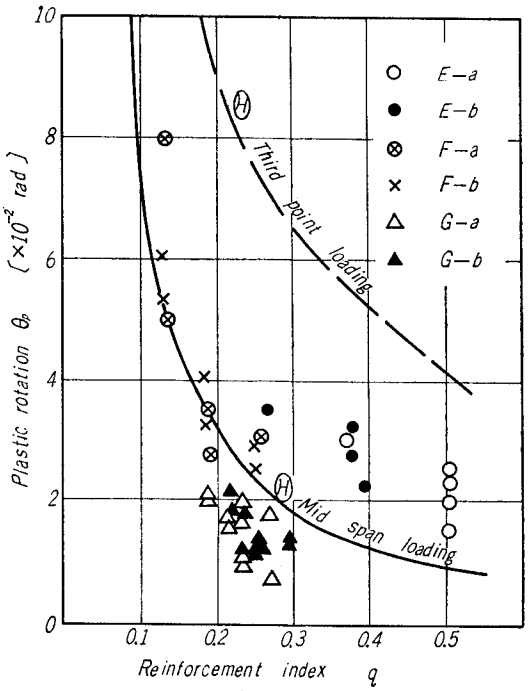

Fig. 5. θ_p versus q relationship of prestressed concrete.

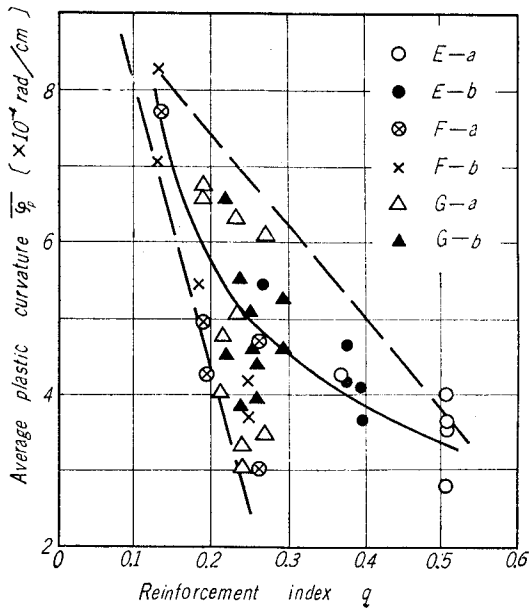

Fig. 6. Average plastic curvature of hinge section versus q curve (prestressed concrete).

point loading (Group E, F), the plastic hinge length is longer than in the mid-span loading (Group G). Therefore the average plastic curvature over the plastic hinge section, $\bar{\varphi}_p$, is calculated. That is, $\bar{\varphi}_p$ is defined as θ_p/l_p where θ_p is the rotation capacity of the plastic hinge and l_p is the hinge length taken as in Fig. 3-a. The relation of $\bar{\varphi}_p$ and q is shown in Fig. 6.

The ratio of the plastic rotation θ_p' at 80 to 90 per-cent level of ultimate load to the ultimate plastic rotation θ_p seems to be independent upon q value, for instance, at 90 per cent of ultimate load the ratio θ_p'/θ_p is about 0.5 to 0.8 in Group F and about 0.3 to 0.4 in Group G.

In this series, too, the rotation capacity of plastic hinge is decreased with the increasing steel ratio. Magnitude of prestress introduced seem to have no appreciable effect on the rotation capacity so long as the steel ratio remains the same. In the doubly reinforced beam (Group G), the rotation capacity seems to be effected not so greatly by the variation in steel ratio and concrete strength.

Fig. 5 shows a similar relation to Fig. 4 for the reinforced concrete, but gives a considerablly smaller value of θ_p corresponding

to the same value of q. This discrepancy may be due to the difference between the stress-strain properties of the prestressing bar, and the usual mild steel bar rather than the plastic extensibilities of "the two types of" concretes used.

The average plastic curvature $\bar{\varphi}_p$ decreases with increasing q, and the $\bar{\varphi}_p \sim q$ curve shows a similar relation to the $\theta_p \sim q$ curve. But $\bar{\varphi}_p$ is very small and about 10 to 20 per-cent of that was found in the reinforced concrete beams with same reinforcement index q.

3.4. Series III - Tests for reinforced concrete continuous beams

3.4.1. Fabrication of specimens and test procedure—Three groups totalling ten kinds of continuous beams, H, I and J, each corresponding to simple beam Group B, C and D in **3.2.**, were made and tested as two-span continuous beams with mid span loading on each span.

In Group I and J, the load cell was used under each of the supports to determine the process of moment redistribution.

3.4.2. Results of tests[2),3)]—When loads are applied to a two span continuous beam having constant section on the middle points of both spans, the moment diagram becomes shown as in Fig. 7-b. With the increase of load P, the maximum moment is reached at the intermediate support C and is equal to the yield moment of that section M_{p1} (Fig. 7-c). If a plastic hinge does not yield in this section the structure fails instantaneously and Fig. 7-c shows the final moment diagram. Whereas if a plastic hinge yields in the section, the moment at the support C remains constant and the mid span moment grows with increasing load until it reaches the resisting moment of the mid-span section M_{p2}. Finally the moment diagram becomes shown as in Fig. 7-d. When the moments at the support C and at the mid-span reach the resisting moments of the particular sections, three plastic hinges being produced, the continuous beam fails as a whole.

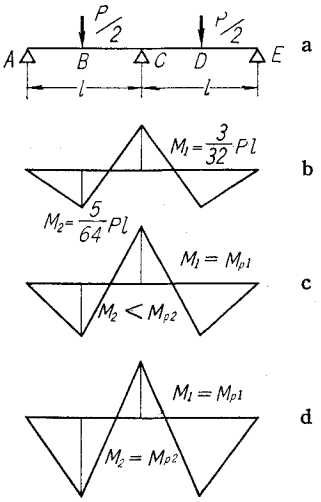

Fig. 7. Moment distribution and plastic hinges yielded.

In a concrete structure, however, it is quite doubtful whether the last hinges are yielded to the full extent at the failure of the structure, even if the first hinge has been completely produced. To examine this problem, the actual ultimate loads were compared with those theoretical values. As the resisting moments of the sections, the measured yield- M_{sy} and the maximum- M_{su} and the calculated moment M_{st} of the corresponding simple beam were used. The theoretical moment M_{st} was calculated from Equation (8).

Table 2. Results of tests in Series III

No. of Specimens	1	2	3	4	5	6	7
	$M_{max}=M_{p1}$	All Hinges yielded			based on P_{su}		q_1
	P_u/P_{su}	P_u/P_{sy}	P_u/P_{su}	P_u/P_{st}	α	β	
H-a-1	1.71	1.61	1.51	1.67	1.00	1.13	0.145
2	1.30	1.24	1.15	1.43	1.00	1.13	0.162
3*	0.97	0.91	0.86	0.99	0.00	1.13	0.202
H-b-1	1.34	1.27	1.16	1.35	1.00	1.13	0.144
2	1.20	1.13	1.06	1.27	1.00	1.13	0.175
3*	0.96	0.88	0.82	0.94	0.00	1.13	0.199
I -a-1	1.46	0.89	0.82	0.78	0.60	1.76	0.270
I -a-2	1.83	0.95	0.90	0.97	0.81	2.02	0.276
J -a-1	1.25	0.74	0.70	0.77	0.32	1.79	0.270
J -a-2	1.51	0.92	0.85	0.96	0.66	1.77	0.244

* failed in shear

$$M_{st}=\left\{\left(1-\frac{q}{2}\right)q+k_c p'(1-d_c')\frac{\sigma_y'}{\sigma_c}\right\}\sigma_c bd^2 \quad \cdots\cdots (8)$$

The ratios of the actual ultimate loads to the theoretical values are shown in Table 2. Column (1) in Table 2 shows the ratio in case where the continuous beam is assumed to fail at $M_{max}=M_{p1}$ without any plastic hinge being produced (see Fig. 7-c). Columns (2)-(4) give the ratios in the case where plastic hinges are assumed to yield to a full extent. In the latter case the ultimate load is calculated by Eq. (9).[4]

$$P=(4M_{p1}+8M_{p2})/l \quad \cdots\cdots (9)$$

where M_{p1}: ultimate resisting moment of the first hinge section

M_{p2}: ultimate resisting moment of the second hinge section

Fig. 8 shows one example of the load versus bending moment rela-

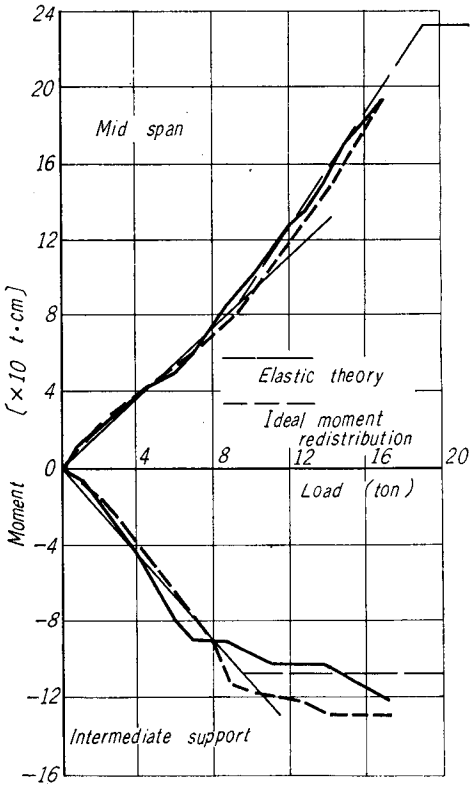

Fig. 8. Load versus moment relationship of reinforced concrete beam (J-a-1).

tionship at the intermediate support and the mid-span. Full straight lines show the theoretical values by the elastic analysis and broken lines represent the ideal moment redistribution curves based on M_{sy}.

In this series of test, some specimens failed from shear compression, whereas none of the corresponding simple beams failed in shear. Shear failure, however, is out of the scope of this study now.

It is clearly shown from column (1) in Table 2 that all specimens except those broken by shear could carry load far beyond the state illustrated in Fig. 7-c, especially so when the resisting moments of the critical sections at the support (C) and at the mid-span (B or D) are different greatly.

Specimens of Group H failed after all of the plastic hinges had been yielded and the internal bending moment had been completely redistributed. In this case, the actual ultimate loads were best agreed with the values estimated by using the ultimate strength M_{su} of the corresponding simple beams. The values estimated by using the yielding moment M_{st} of the section given by Eq. (8) are most conservative. The beams of Groups I and J, in which the difference between the resisting moments of the two critical sections is very large, have also sufficient load carying capacity even beyond the stage shown in Fig. 7-c. However, columns (2) to (4) in Table 2 give smaller values than 1.0. This fact shows that the beams failed so that the redistribution of internal moment was not fully developed, the yield of plastic hinges being incomplete.

The aspect of moment redistribution is clearly shown in Fig. 8. The moment distribution seems almost purely elastic at low load. When the external moment at the first hinge section exceeds the yield moment of that section, the curve deviates from the straight line and the moment at the section remains almost constant. On the other hand the mid span moment increases as the increase of load along the theoretical moment redistribution curve. The redistribution process coincides closely with that shown in the ideal elastic-plastic materials.

Now a parameter α is considered to express the degree of the development of the second plastic hinge. If we assume that α is given quite correspondingly to the degree of the internal moment redistributed to the last hinge section, parameter α is expressed as follows,

$$\alpha = (P_u - P_1)/(P_2 - P_1) \qquad \cdots\cdots\cdots\cdots (10)$$

where P_u is the measured ultimate load and P_1, P_2 are the loads calculated for the state shown in Fig. 7-c, 7-d, respectively. A parameter β is also used for representing the increment of theoretical load from the finish of the first hinge to that of the second hinge, that is, β means the ratio of P_2 to P_1.

The degree of the yield of plastic hinge are listed in Table 2. Parameter α decreases with increasing β or the reinforcement index, q_1, of the first hinge section.

In group J in which deformed bars were used as the reinforcement, α is smaller than the group I in which plain bars were used. It cannot be explained in this test why such difference in α was found between the both kinds of steel. It may be considered that there may be some influence of bond strength or slip on the degree of the yield of plastic hinge.

3.5. Series IV - Test for prestressed concrete continuous beams

3.5.1. Fabrication of specimens and test procedure—Six kinds of continuous beam specimens were made, the section of which are chosen so as to correspond to those of Group G in Series II. The specimens were tested as a two-span continuous beam by loading on each mid span and the test procedure was quite same as taken in the test series III.

3.5.2. Results of tests—The results of test are listed in Table 3 in the same expression as in Table 2. The relations of applied load to the moments at the intermediate and at the mid span are represented in Fig. 9. The theoretical curves in Fig. 9 are obtained in the same manner as in Fig. 8.

It was found from the measurements of strains of sections along the beam length that all sections except under the loading points and at the intermediate support remained almost in an elastic state up to the failure of the beams. Hence the plastic rotation at the intermediate support θ_{pc1} and at the mid-span θ_{pc2} can be determined from the plastic curvature of the above particular sections, respectively, and were compared to the corresponding plastic rotations of the simple beams.

Table 3 clearly shows that measured values are about 20 to 70 percent larger than the values estimated under the assumption of non-yielding of plastic hinge (column (1)). Especially the deviation is larger with increasing β. The values calculated by using the strength P_{su} of the corresponding simple beams under the assumption of

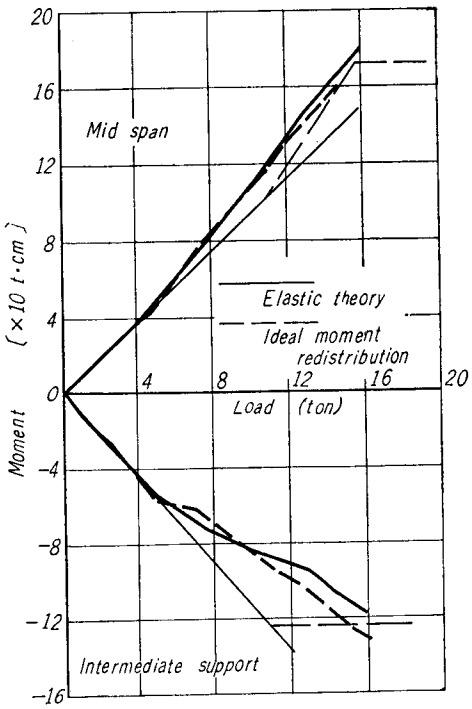

Fig. 9. Load versus moment relationship of prestressed concrete beam (K-b-3).

Table 3. Results of tests in Series IV.

No. of Specimens	1	2	3	4
	No hinge	All Hinges yielded		based on P_{su}
	P_u/P_{su}	P_u/P_{sy}	P_u/P_{su}	β
K-a-1	1.26	1.53	1.13	1.13
2	1.50	1.53	1.07	1.40
3	1.74	1.48	1.13	1.54
K-b-1	1.20	1.54	1.06	1.12
2	1.39	1.41	1.09	1.24
3	1.49	1.38	1.04	1.43

perfect developement of plastic hinges, coincide closely with the measured values, the difference being generally less than 10 percent (column (3)). It can be concluded so far as this test is concerned that the redistribution of moment is completely done even on prestressed concrete members. The values estimated from the yield moment M_{sy} of the corresponding simple beam do not show good agreement with the measurements (column (2)). Consequently, the definition of yield moment in Fig. 2 may be used limitedly only for calculation of plastic rotation.

It is very interesting to compare the process of moment redistribution in prestressed and reinforced concrete. In case of prestressed concrete beams, the observed redistribution at higher load does not follow to the ideal redistribution curve. Redistribution begins when initial cracks are formed, and developes gradually with increasing load up to the failure of beam. This is quite contrary to the reinforced concrete beams showing an approximately ideal redistribution process.

Fig. 10 shows the ratio Φ of the ultimate plastic rotations of continuous beam to that of simple beam in terms of β. At the intermediate support, where a plastic hinge is formed at first, Φ draws nearer to 1.0 and tends even to exceed 1.0 as the increase of β. If β is larger than the critical β_0 giving $\Phi=1.0$, the plastic rotation required would be so large that failure of beam due to the crushing of concrete in the compression zone would precede. This means that the yield of plastic hinge at this section is considered to remain actually incomplete when $\beta>\beta_0$. The value of critical β_0, however, can not be determined due to the limited data available in this test.

3. 5. 3. Considerations on imperfect plastic hinge—In the plastic design theory, generally, the capacity of plastic rotation is considered only about the first hinge section and not about the last hinge section. In a prestressed concrete member

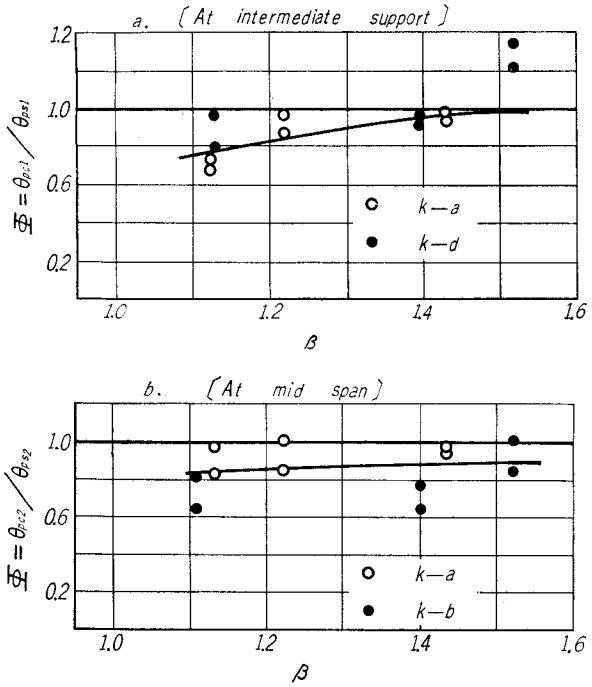

Fig. 10. The ratio of plastic rotation of continuous beam and simple beam
a. (at intermediate support)
b. (at mid span)

the plastic rotation begins to occur in the last hinge section before the external moment of the first hinge section has reached the yield moment. For the perfect developement of the moment redistribution, sufficient magnitude of plastic rotation should be performed in all critical sections. The relation of plastic rotations in the critical sections are obtained as follows. In case of the loading as shown in Fig. 11-a, if the plastic rotations occur concentratedly in their loaded sections, the curvature ϕ and the angle change θ are as shown in Fig. 11-b. ϕ_1 and ϕ_2 are the elastic curvatures of C and D (B) sections respectively. From condition of compatibility the following equations can be derived.

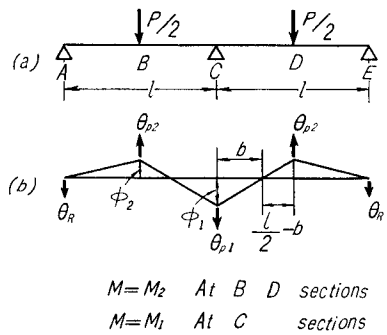

Fig. 11. Distribution of curvature and rotation in continuous beam.

$$\theta_R+\frac{1}{2}\theta_{p1}-\theta_{p2}+\frac{1}{2}b\phi_1-\frac{1}{2}(l-b)\phi_2=0 \quad \cdots\cdots (11)$$

$$l\cdot\theta_R \quad -\frac{1}{2}l\theta_{p2}+\frac{1}{6}b^2\phi_1-\frac{1}{12}(3l+2b)(l-b)\phi_2=0 \quad \cdots\cdots (12)$$

Eliminating θ_R and by using $b=l/2(1+r)$

$$\theta_{p1}=\theta_{p2}+\frac{l}{12(1+r)^2}\{(2r+1)(3r+2)\phi_2-(6r+5)\phi_1\} \quad \cdots\cdots (13)$$

where r is the ratio of resisting moment of two sections; i.e. $r=M_{r2}/M_{r1}$. The elastic term can be written as $\phi(r)$. Then

$$\theta_{p1}=\theta_{p2}+\phi(r) \quad \cdots\cdots (14)$$

Hence

$$\theta_{p2}/\theta_{p1}=1-\phi(r)/\theta_{p1} \quad \cdots\cdots (15)$$

The value of $\phi(r)$ increases with increasing r. It is, however, so small that θ_{p2} influences remarkably the necessary plastic rotation of the first hinge section. Hence, when the rotation of the second hinge section is much larger than θ_{p1}, the moment redistribution may become imperfect even though the rotation capacity of the first hinge section is larger enough. For the full development of moment redistribution on concrete members, the following factors should be favorable; (a) large rotation capacity of the first hinge section, (b) small rotation capacity of the second hinge section, (c) small β or r, which is the ratio of resisting moments of the two sections.

4. Summary

The results from this investigation may be summarized as follows;

(1) The plastic rotation is influenced by the concrete strength, the steel ratio and the yield stress of steel. Plastic rotation decreases with the increasing of reinforcement index q. In the case of reinforced concrete beams, the calculated values derived from the energy theory indicate nearly the minimum of all the measured values.

(2) In case of prestressed concrete beam, the yield point of beam is not definite. The plastic rotation, however, can also be calculated just as in case of reinforced concrete beam under some proper assumptions, and the general relation between the plastic rotation to the reinforcement index is similar to that of reinforced concrete beam. But for the same value of q, the plastic rotation thus determined is less than a half to one third of that of reinforced concrete beams.

(3) It is useful for studies on the plastic hinge to use the average rotation of section $\bar{\varphi}_p$ over the region of the plastic hinge, because the difference in loading manner is excluded. $\bar{\varphi}_p$ also decreases with the increase of q, but problems still remain in determining the region of the plastic hinge l_p.

(4) In the continuous beam, the redistribution of moment was recognised. When the parameter β is smaller, the plastic hinges are fully developed in the prestressed concrete beam as well as in the reinforced concrete beam. However,

when β becomes larger, the beam fails when the last hinge has not completely been developed. That is, in this case, the yield of plastic hinge remains incomplete.

(5) The moment redistribution diagrams in the reinforced concrete beam coincide with those found in the ideal elastic-plastic materials. The curves of prestressed concrete beam, however, deviate considerably from the theoretical curve of the elastic-plastic materials, and the moment redistribution occurs gradually after cracking is caused in the beam.

(6) Rigorously speaking, the ideal moment redistribution process may not be expected in a concrete structure, and we must take into consideration the amount of plastic rototion of the last hinge section in addition to that of the first hinge section in the ultimate design of concrete structures.

This paper describes the results of the experimental study about the yield of plastic hinge. The study is limited to the particular loading conditions, but it may be extended rather easily to other conditions. The authors hope it will be helpful for the establishment of plastic design theory of concrete structures.

References

1) M. Yamada : "Drehfähigkeit plastischer Gelenke in Stahlbetonbalken" Beton und Stahlbau, 53 Jahrgang, Heft 4, Apr. 1958
2) George C. Ernst : "Moment and shear redistribution in two-span continuous reinforced concrete beams". Journal of ACI. Vol. 30, No. 5, Nov. 1958
3) W. W. L. Chan : "The rotation of reinforced concrete plastic hinge at ultimate load". Magazine of Concrete Research, Vol. 14, No. 41, July 1962
4) Philip G. Hodge, Jr. : "Plastic analysis of structures" McGraw Hill Book Co. 1959